

A large-scale photonic node architecture that utilizes interconnected OXC subsystems

Yuto Iwai,^{*} Hiroshi Hasegawa and Ken-ichi Sato

Department of Electrical Engineering and Computer Science, Nagoya University Furo-cho, Chikusa-ku, Nagoya, 464-8603, Japan

^{}y_iwai@echo.nuee.nagoya-u.ac.jp*

Abstract: We propose a novel photonic node architecture that is composed of interconnected small-scale optical cross-connect subsystems. We also developed an efficient dynamic network control algorithm that complies with a restriction on the number of intra-node fibers used for subsystem interconnection. Numerical evaluations verify that the proposed architecture offers almost the same performance as the equivalent single large-scale cross-connect switch, while enabling substantial hardware scale reductions.

©2012 Optical Society of America

OCIS codes: (060.1155) All-optical networks; (060.4251) Networks, assignment and routing algorithms.

References and links

1. K. Sato and H. Hasegawa, "Optical networking technologies that will create future bandwidth-abundant networks," *JOSN* **1** (2), A81-A93 (2009).
2. K. K. Kubota, "Beyond HDTV-ultra high-definition television system," Presented at 2nd Multimedia Conference 2006 (2006).
3. A. L. Chiu, G. Choudhury, G. Clapp, R. Doverspike, M. Feuer, J.W. Gannett, G. Kim, J. Klinecicz, T. Kwon, G. Li, P. Magill, J.M. Simmons, R.A. Skoog, J. Strand, A. Lehmen, B.J. Wilson, S. Woodward, Dahai Xu, "Architectures and protocols for capacity efficient, highly dynamic and highly resilient core networks," *JOSN* **4** (1), 1-14 (2012).
4. S. Liu and L. Chen, "Deployment of carrier-grade bandwidth-on-demand services over optical transport networks: A Verizon experience," in Proc. OFC/NFOEC 2008, NThC3 (2008).
5. V. Shukla, D. Brown, C. J. Hunt, T. Mueller, and E. Varma, "Next generation optical network - enabling dynamic bandwidth services," in Proc. OFC/NFOEC 2007, NWB3 (2007).
6. S. Beckett and M. A. Lazer, "Optical mesh service-service strategy capitalizing on industry trends," Presented at OIF Workshop (2006).
7. P. Pagnan and M. Schiano, "A λ switched photonic network for the new transport backbone of Telecom Italia," PS 2009, TH12-1 (2009).
8. S. L. Woodward, S. Woodward, "What is the value of the flexible grid network?," OFC/NFOEC 2012 WS (2012).
9. H. Zang, J. P. Jue, L. Sahasrabudde, S. Ramamurthy, and B. Mukherjee, "Dynamic lightpath establishment in wavelength-routed WDM networks," *IEEE Commun. Mag* **39** (9), 100-108 (2001).
10. X. Chu, B. Li, "Dynamic routing and wavelength assignment in the presence of wavelength conversion for all-optical networks," *IEEE/ACM Trans. Netw.* **13** (3) (2005).
11. M. Allalouf, Y. Shavitt, "Centralized and distributed algorithms for routing and weighted max-min fair bandwidth allocation," *IEEE/ACM Trans. Netw.* **16** (3) (2008).
12. Y. Yoo, S. Ahn, C.S. Kim, "Adaptive routing considering the number of available wavelengths in WDM networks," *JSAC* **21** (8) (2003).

13. B. Zhang, J. Zheng, H.T. Mouftah, "Fast routing algorithms for Lightpath establishment in wavelength-routed optical networks," *JLT* **26** (13) (2008).
 14. A. Jukan, G. Franzl, "Path selection methods with multiple constraints in service-guaranteed WDM networks," *IEEE/ACM Trans. Netw.* **12** (1) (2004).
 15. H. Ohno, H. Hasegawa, K. Sato, "A dynamic and quasi-centralized RWA method for optical fast circuit switching networks employing route pre-prioritization," *OSN* **8**, 242–248 (2011)
 16. Y. Iwai, H. Hasegawa, and K. Sato, "Large-Scale Photonic Node Architecture that Utilizes Interconnected Small Scale Optical Cross-connect Sub-Systems," *ECOC 2012, We.3.D.3* (2012)
 17. R. Inkret, A. Kuchar, and B. Mikac, "Advanced infrastructure for photonic networks extended final report of COST 266 action," Faculty of Electrical Engineering and Computing, University of Zagreb, (2003), http://www.ikr.uni-stuttgart.de/Content/Publications/Archive/Ga_COST266_ExtendedFinalReport_36355.pdf.
 18. A. Allasia, V. Brizi, M. Potenza, "Characteristics and trends of telecom italia transport networks," *Fiber Integrated Opt* **27** (4), 183–193 (2008).
 19. J. Simmons "*Optical network design and planning*," Springer (2008)
 20. T. Niwa, H. Hasegawa and K. Sato, "Compact wavelength tunable filter fabricated on a PLC chip that construct colorless/directionless/contentionless drop function in optical cross-connect," *OFC/NFOEC 2012, OTh3D* (2012).
-

1. Introduction

The present IP traffic increase, ~40 % a year, will yield 10 times more traffic in seven years and 100 times in 14 years, which may be further enhanced with the introduction of new wavelength services, since dynamic wavelength services that include ultra-/super- high definition video (72 Gbps per channel) distribution [1, 2] among TV broadcasting stations or headends, and future advanced wavelength services [3-6] are envisaged. The explosion in traffic will force a rapid increase in the number of wavelength paths and that of fibers between adjacent nodes as indicated in [7], and the importance of developing a large scale ROADM/OXC has been emphasized [8]. To create large scale OXCs (multi-degree ROADMs) that utilize WSSs, a large port count WSS is required. However, the highest port count commercially available at present is limited to 20+. It will be very difficult to 100+ ports in the near future. One straight-forward way to increase the port count is to cascade WSSs. If we use 1x9 WSSs, a two stage architecture yields 1x81 WSS, however, it requires 10 1x9 WSSs and the loss is twice that of the unit WSS. It is not practical in terms of cost and loss.

This paper proposes a large port count OXC that consists of multiple OXC-subsystems that are realized with smaller cost-effective WSSs; they are interconnected by a limited number of fibers. The architecture offers good modular growth capability that allows the cost-effective introduction of large-scale OXCs even at the outset. The proposed architecture permits intra-node contention to occur due to a shortage of capacity or from wavelength collision in optical fibers that connect each OXC-subsystem. This

is in addition to the inter-node wavelength collision in fibers connecting neighboring node OXCs that we usually consider in the context of RWA (Routing and Wavelength Assignment) in designing wavelength-routed optical networks. Further, intra-node contention and inter-node contention are strongly related, and hence optimization is necessary as a whole. In other words, the performance of the OXC cannot be evaluated as a stand-alone system, but should be evaluated in conjunction with the network control algorithm. Several dynamic wavelength path operation algorithms have been studied (for example, [9-15]), where conventional OXCs with no routing restriction are assumed. We propose here a novel dynamic network control algorithm that makes best use of the proposed OXC. Numerical experiments prove the combination of proposed node architecture and algorithm can greatly reduce the necessary hardware scale, the total number of WSSs, while the performance offset from large single system OXCs (constructed with large port count WSSs or with utilizing cascaded multi-stage smaller WSSs) is marginal with the same number of total input (output) fibers. A preliminary version of this work was presented at an international conference [16].

2. Proposed node architecture

The proposed node architecture is shown in Fig. 1. It consists of small ($m \times n$) interconnected OXCs (conventionally $m=n$), that are bridged by a limited number of fibers. Hereafter we call these small OXCs “OXC-subsystems”. These OXC-subsystems can be cost-effectively realized with low degree WSSs and star-couplers (Fig. 2). Please note that the degree of the OXC-subsystem is small, so star-couplers can be applied on either side of the OXC. Using large degree WSSs to create a large degree OXCs, demands that WSSs be placed at both input and output sides of the OXC to eliminate the large optical losses of star-couplers, which doubles the number of WSSs needed.

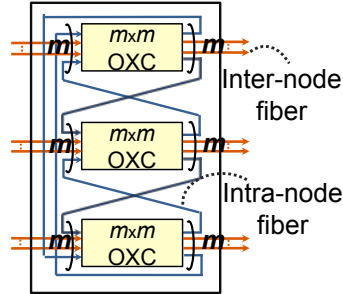


Fig.1 Proposed OXC node architecture

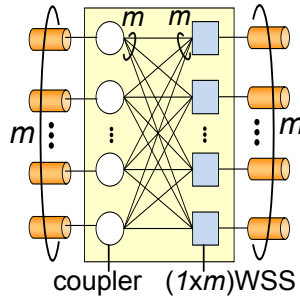


Fig.2 WSS based OXC architecture

Although various interconnection architectures for connecting OXC-subsystems exist, we assumed one of the simplest interconnection architectures, the ring-like connection shown in Fig. 4, where only adjacent OXC-subsystems are bridged. Fig. 3 shows a connection example for 2, 3 and 4 OXC-subsystems. The number of input/output fibers of a proposed node increases with OXC-subsystem number. For example, if each OXC-subsystem is $D \times D$ and each pair of adjacent OXC-subsystems is bridged by a pair of fibers (bi-directional), then the number of input (or output) fibers f_{in} is given by

$$f_{in} = f_{out} = \begin{cases} D & \text{if } l = 1 \\ 2(D-1) & \text{if } l = 2 \\ l(D-2) & \text{if } l \geq 3 \end{cases} \quad (1)$$

where l is the number of OXC-subsystems.

Regarding routing capabilities between OXC-subsystems, the number of wavelength paths that have the same wavelength and routed from one OXC-subsystem to its adjacent one is bounded by the number of fibers connecting them. Numerical experiments show that our dynamic network control algorithm, which considers this limitation, almost matches the throughput obtained with an equivalent single layer large scale OXC.

If LCOS based WSSs are utilized, the proposed architecture naturally accommodates not only wavelength paths on the ITU-T fixed grid, but also elastic/flex-grid optical paths, however, for simplicity, we focus on the fixed grid case through this paper.

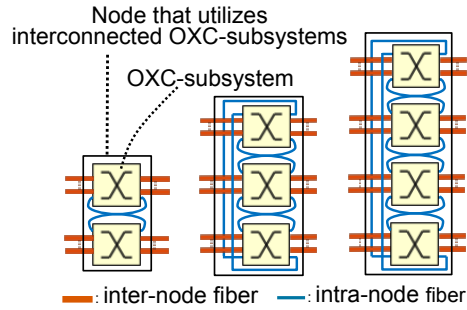


Fig. 3 Connection between OXC-subsystems

3. Intra-node blocking aware dynamic optical path control algorithm

We propose here a dynamic path control algorithm to accommodate dynamic traffic demands in networks that utilize the proposed OXCs. The goal of this algorithm is to suppress the blocking probability increase possible compared to conventional networks. In this section, we assume that no wavelength conversion is provided and all link distances are the same for simplicity. Here we limit the number of intra node fibers traversed by a wavelength path; the bound is denoted by F_{intra} . For example, when $F_{intra} = 2$, each wavelength path can traverse two intra node fibers, or three OXC-subsystems, in one node, or can traverse one intra node fiber, or two OXC-subsystems, in each of the two nodes. We also introduce a parameter called hop slug, the hop increment bound from the shortest hop, to avoid lengthy detouring. For a given topology and fibers, the following algorithm is used to set-up each path demand request. Because of the space limitation, we simply outline the algorithm.

<Dynamic control algorithm for networks that utilize proposed OXCs>

Step0: If an existing path request terminates, tear down the path immediately and terminate. Otherwise, i.e. if a path setup request arrives, go to Step 1.

Step1: For each wavelength, create an auxiliary graph (see Fig. 4) where each node stands for one interconnected OXC-subsystem and links for inter/intra node fibers connecting OXC-subsystems where the wavelength is not used.

Step2: Find a route that minimizes the number of inter-node links traversed while keeping that of intra-node links traversed equal to or less than F_{intra} . If the node hop count on the found route is larger than the sum of the shortest hop count and the hop slug, exclude the route from the route candidates. If there are multiple optimal routes, randomly select one. If there is no route candidate, block the request.

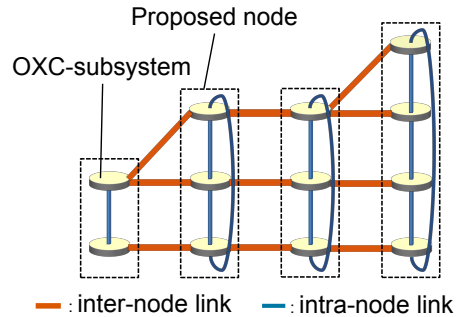
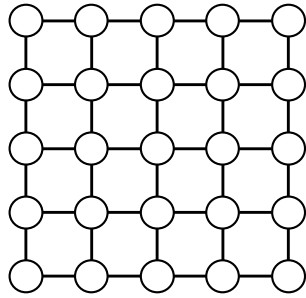


Fig. 4 A layered auxiliary graph

4. Numerical experiment

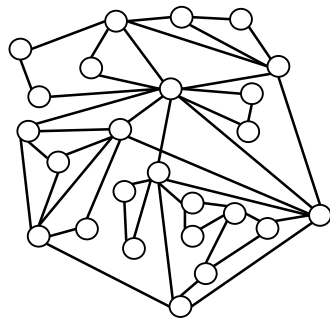
The numerical experiment uses the following parameters. Physical network topologies are the 5x5 poly-grid network, the Pan-European network COST266 [17], France network and Italy network [18] (Fig. 5) where link length is set constant. Characteristics of those network models are summarized in Table 1. Wavelength conversion is not considered, and each fiber can accommodate 80 wavelengths. We assume that the traffic demand is uniform and randomly distributed and is represented as the average number of wavelength paths between each node pair. The generation of path setup demands follows a Poisson process. The holding time of each connection follows a negative exponential distribution. For the proposed node architecture, we assume that the OXC-subsystem size is 9x9 (namely, 1x9 WSSs are utilized) and each pair of adjacent OXC-subsystems is bridged by one pair of fibers (one input and one output fiber as seen in Fig. 1). The hop slug is set at 2 for both the proposed and conventional algorithms [19]. The conventional algorithm is for a network that utilizes single large OXC at each node in which no intra-node blocking occurs. Additional WSS ports that may be utilized by traffic that drops from each input fiber at a node are not considered for simplicity, since the add/drop part is common to all architectures. We have recently developed a very compact tunable filter using PLC technology [20]. We believe that the technology provides one of the efficient ways to realize C/D/C add/drop part, however, this is out of scope of this study.



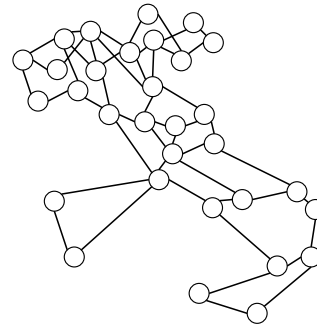
5x5 poly-grid network



Pan-European network COST266



France network



Italy network

Fig. 5 Experimental physical network topology

Table 1 Characteristics of 5x5 poly-grid network, COST266 network, France network and Italy network

		Network topology			
		5x5	COST266	France	Italy
Number of nodes		25	26	25	31
Node degree	Min	2	2	2	2
	Max	4	8	10	5
	Ave	3.20	3.92	3.60	3.12
Number of Links		40	51	45	49
Number of shortest hops	Min	1	1	1	1
	Max	8	6	5	9
	Ave	3.33	2.76	2.62	3.72

The number of interconnected OXC-subsystems within each node is determined by the necessary number of input/output fibers to/from the adjacent nodes. We firstly perform static network design for network with conventional single OXC node at a certain traffic volume and find necessary number of OXC input/output fibers at each node. We then determined the number of interconnected OXC-subsystem so that the same number of the input/output fibers can be provided with the proposed architecture. For example, when the number of input (output) fibers is 20, then 3 ($\lceil 20 \div 7 \rceil$; each OXC-subsystem offers 7 ($\lceil 9 - 2 \rceil$ inter-node fibers) OXC-subsystems are necessary. Therefore, we applied a static network design algorithm that assumes conventional single OXC nodes and evaluated necessary node scale and number of fibers on each link for 20 different traffic distributions. The conventional single OXC node represents the node that consists of a single large OXC or the equivalent that has no intra-node blocking.

For each node, we derived the maximum number of fibers in 20 trials and then the number of interconnected OXC-subsystems for each node that is necessary and sufficient to connect the maximum fibers. Depending on the network topology and a node in each network, the number of input/output fibers from/to adjacent nodes differs. When the average number of wavelength paths between each node pair was 7, the maximum number of input/output fibers among all nodes was 15 in the 5x5 poly-grid topology, 21

in the COST266 topology, 41 in the France topology and 34 in the Italy topology.

The number of fibers on each link of the networks that used the proposed node was also determined through static network design; 10 different traffic distributions were considered where the average number of wavelength paths between each node pair was 7. The routing performance is slightly different from that of a conventional single OXC node, and therefore, a dedicated network design algorithm is needed to determine suitable intra-node subsystem connections; different connection patterns exist, each of which consists of a different number of subsystems.

We compared the performance of a network that uses the proposed nodes to a network that uses the conventional nodes. Both networks have the same number of inter-node fibers. The simulation results are averaged over 10 different runs.

Comparisons of blocking ratio versus traffic intensity in the four different networks are shown Fig. 6, 7, 8 and 9. The value of F_{intra} was set at 0, 1, 2 and 4 for the network with the proposed node. The horizontal axis plots traffic intensity, normalized by traffic volume where the average number of wavelength paths between each node pair is 7. These figures show that increasing F_{intra} reduces the blocking ratio. In other words, larger F_{intra} offers better network performance. When the target of blocking ratio was 0.1%, all proposed networks with $F_{intra} = 4$ can accommodate almost the same traffic as the conventional network.

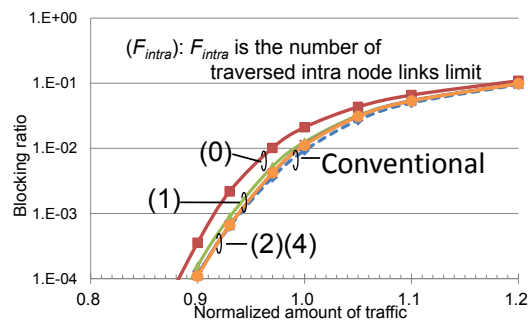


Fig. 6 Blocking performance comparisons in networks with conventional and proposed nodes (5x5 poly-grid network)

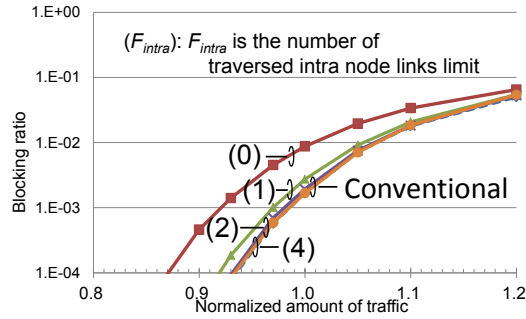


Fig. 7 Blocking performance comparisons in networks with conventional and proposed nodes (Pan-European network COST266)

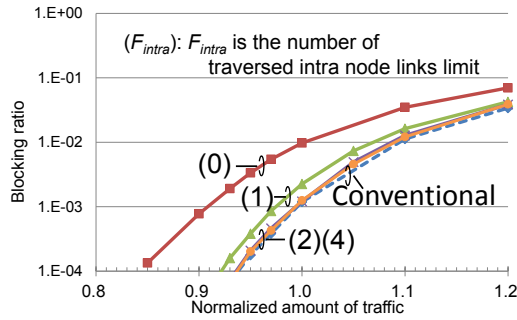


Fig. 8 Blocking performance comparisons in networks with conventional and proposed nodes (France network)

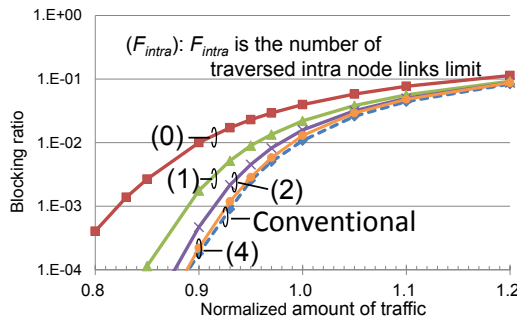


Fig. 9 Blocking performance comparisons in networks with conventional and proposed nodes (Italy network)

We then investigated routing performance variations on network scales. We tested 5x5, 6x6 and 7x7 poly-grid networks where the average number of wavelength paths between each node pair was 7. Table 2 summarizes the characteristics of the 5x5, 6x6 and 7x7 poly-grid networks with proposed nodes. The corresponding blocking performance results are presented in Fig. 6, Fig. 11 and Fig. 12. These results show that the routing performance of the network with proposed nodes slightly deteriorates as network scale increases. For example, in the 5x5 topology with $F_{intra} = 2$, the proposed node architecture attains almost the same normalized traffic ratio as the conventional node architecture if the target of blocking ratio is 0.1%. On the

other hand, for the 6x6 topology with $F_{intra} = 2$, the normalized traffic ratio is degraded by 2%. Moreover, for the 7x7 topology with $F_{intra} = 2$, the degradation becomes 4%. This performance degradation stems from the increase in the number of OXC-subsystems within the proposed nodes and the increase in the average number of hops. However, even with 6x6 and 7x7 topologies, $F_{intra} = 8$ allows the performance of the proposed network to match that of the conventional network.

Table 2. Characteristics of $(N \times N)$ poly-grid networks with the proposed nodes ($N = 5, 6, 7$)
the average number of wavelength paths between each node pair = 7

		Network topology		
		5x5	6x6	7x7
Number of nodes		25	36	49
Node degree	Min	2	2	2
	Max	4	4	4
	Ave	3.20	3.33	3.43
Number of Links		40	60	84
Number of shortest hops	Min	1	1	1
	Max	8	10	12
	Ave	3.33	4.00	4.67
Number of OXC-subsystems within each proposed node	Min	1	1	1
	Max	2	4	6
	Ave	1.36	2.44	3.59
Maximum number of input (output) fibers among all nodes		15	25	38

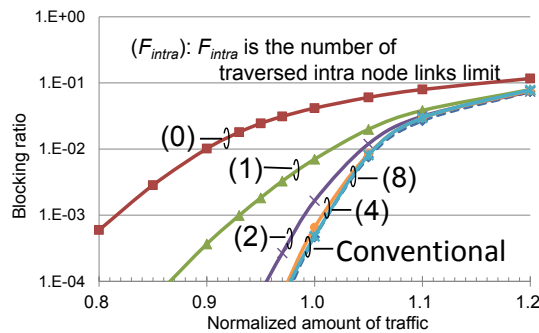


Fig. 10 Blocking performance comparison with conventional nodes and proposed nodes (6x6 poly-grid network)

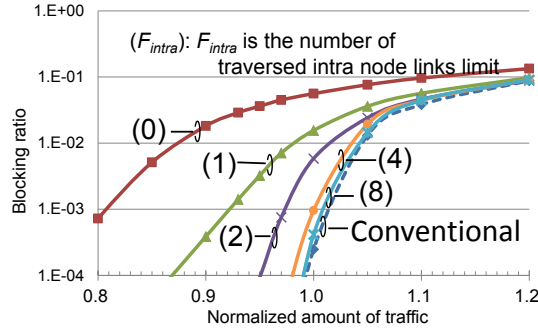


Fig. 11 Blocking performance comparison with conventional nodes and proposed nodes (7x7 poly-grid network)

We evaluated hardware scale of OXCs in terms of necessary number of 1x9 WSSs for each network. In the conventional network, large scales WSSs are realized by cascading small WSSs (1x9 WSSs) as shown Fig 12. The architecture of both proposed and conventional OXC assumed the broadcast-&-select configuration (Fig. 2). The number of WSSs necessary for the four networks tested is shown Fig. 13. Here the average number of wavelength paths between each node pair was set at 7. The vertical axis plots the relative number of 1x9 WSSs; normalized by the number of WSSs necessary in the conventional network. Please note that F_{intra} values do not affect the necessary hardware scale, since the values is just utilized with RWA process, although F_{intra} affects routing performance as shown in Fig. 9-11.

For all networks, the proposed OXC architecture significantly reduces the necessary number of WSSs, ranging from 29.8% for the 5x5 to 49.1% for the Italy network. In Fig. 13, the average number of wavelength paths between each node pair was set at 7 for all the networks. However, the network scales (number of nodes) are different among topologies (see Fig. 6). The larger the number of nodes, the larger the total amount of optical paths, which requires larger OXCs. When the OXC port count increases, the required number of WSSs for the conventional architecture increases much faster than that for proposed architecture. Therefore, the larger network (Italy network) yields larger reduction. To avoid large optical coupler loss in the conventional OXC architecture with broadcast-&-select configuration, the route and select architecture must be adopted. In this case, the hardware reduction achieved with the proposed architecture, which would utilize 9x1 star couplers, is greatly enhanced.

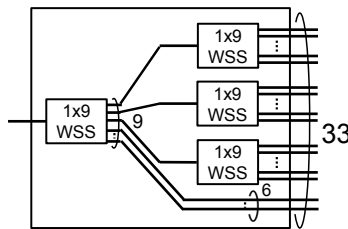


Fig. 12 An example of 1x33 WSS made by concatenating 1x9 WSSs

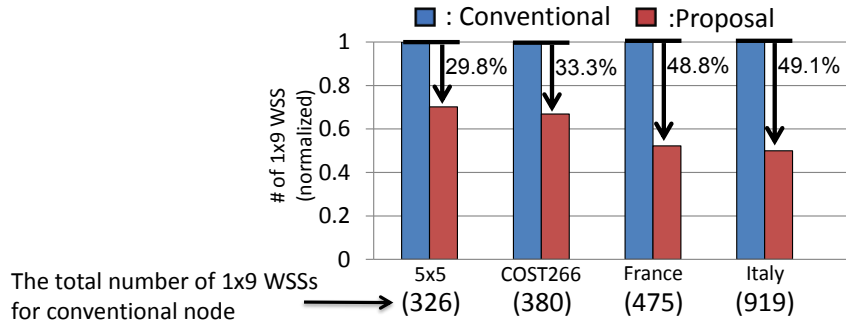


Fig. 13 Hardware scale comparison with conventional networks

5. Conclusion

In this paper, we proposed a novel large scale optical cross-connect switch architecture that consists of interconnected small-scale OXCs. We also developed an efficient dynamic network control algorithm. Numerical experiments demonstrated that networks equipped with the proposed nodes achieve almost the same blocking probabilities as conventional networks, while offering significantly reduced required total switch scale.

Acknowledgement

The work was partly supported by the NICT λ -reach project and KAKENHI (23246072).